# Journal Pre-proof

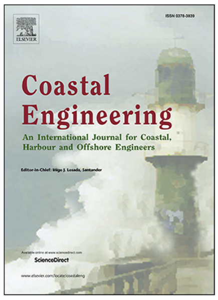


Reduced wave time series for long-term morphodynamic applications

Francesca Scipione, Paolo De Girolamo, Myrta Castellino,
Davide Pasquali, Daniele Celli, Marcello Di Risio

PII: S0378-3839(24)00001-2
DOI: https://doi.org/10.1016/j.coastaleng.2024.104453
Reference: CENG 104453

To appear in: *Coastal Engineering*

Received date : 16 September 2022
Revised date : 9 August 2023
Accepted date : 5 January 2024

Please cite this article as: F. Scipione, P. De Girolamo, M. Castellino et al., Reduced wave time series for long-term morphodynamic applications. *Coastal Engineering* (2024), doi: https://doi.org/10.1016/j.coastaleng.2024.104453.

# Reduced wave time series for long-term morphodynamic applications

Francesca Scipione[a,*], Paolo De Girolamo[a], Myrta Castellino[a], Davide Pasquali[b], Daniele Celli[b] and Marcello Di Risio[b]

[a] Department of Civil, Building and Environmental Engineering (DICEA), Sapienza University of Rome, Rome, Italy
[b] Environmental and Maritime Hydraulic Laboratory "Umberto Messina"(LIam), Department of Civil, Construction-Architectural and Environmental Engineering (DICEAA), University of L'Aquila, L'Aquila, Italy

ARTICLE INFO

*Keywords*:
climate change
long-term shoreline evolution
one-line models
wave forcing

ABSTRACT

Shoreline models have usually been recognized by professionals as the most appropriate tool for reproducing the long-term morphodynamic evolution of the shoreline of sandy beaches. Despite their underlying simplifications, the simulation of shoreline evolution at large temporal and spatial scales may imply significant computational efforts. Hence, to reduce computational costs, many approaches aimed to optimize the size of the input wave datasets have been proposed so far. A simplified novel method to reduce long-term offshore wave series is proposed herein. The rationale of the approach is to build reduced series that induce the same morphodynamic effects in the long-term as the ones induced by the whole, and more computationally expensive, original series. The method is conceived to define offshore reduced time series with the same chronological order of the complete series and is able to represent the bi-modal features of the wave climate. In-depth hydrodynamic and morphodynamic parametric analyses have been performed and it has been demonstrated that the method is capable to get reliable reduced offshore wave time series for reproducing the long-term evolution of sandy beaches with decreased computational costs.

## 1. Introduction

Within the frame of the optimization of long-term planning, the role of simplified one-line models has been shown to be essential for their low computational costs. Despite their simplifications and criticisms raised by many authors (e.g. Cooper and Pilkey, 2004), their use is usual and quite effective to identify areas affected by either shoreline advances or retreats, and aid planners in defining the most appropriate actions for the management of the coastal zone. Indeed, the effectiveness of one-line models often allows the reproduction of different scenarios, which, in turn, is crucial to evaluating the long-term performance of different strategies (e.g. Pasquali and Marucci, 2021) that often rely on the optimization of soft (e.g. Bruun, 1983; Capobianco et al., 2002; Damiani et al., 2011; Fischione et al., 2022), hard (e.g. Stauble and Tabar, 2003; Celli et al., 2019, 2021) or mixed (e.g. Creter et al., 1994; Saponieri et al., 2018; Di Risio et al., 2010) interventions. The main input data for one-line models are at least: initial shoreline configuration, sand characteristics (e.g. mean grain size), and wave parameters (e.g. significant wave height, peak wave period, and wave direction). It is worth reminding that one-line models rely on the assumption that the cross-shore sediment transport effects are negligible with respect to the longshore component (e.g. Larson et al., 1987). Hence, as a consequence,

*Corresponding author
francesca.scipione@uniroma1.it (F. Scipione)
ORCID(s): 0000-0001-8242-5894 (F. Scipione); 0000-0001-6339-472X (.P. De Girolamo); 0000-0002-7119-4901 (.M. Castellino); 0000-0002-1255-3011 (.D. Pasquali); 0000-0003-2656-6531 (.D. Celli); 0000-0002-0382-7615 (.M. Di Risio)

the shape of the cross-shore beach profile remains constant in the long term. A plethora of formulae exists to estimate the longshore sediment transport responsible for the long-term evolution as per one-line model assumptions. Many of them relate the magnitude of the longshore sediment transport to wave parameters at breaking conditions (e.g. U.S. Army Corps of Engineers, 1984; Kamphuis, 1991). Hence, either simplified wave transformation models (e.g. Dally et al., 1985) or wave models with different levels of complexity and reliability (e.g. Holthuijsen et al., 1993; Beltrami et al., 2001) are usually implemented within one-line models to estimate the synthetic parameters of breaking waves. Whatever the type of wave propagation model, the definition of offshore wave time series to be propagated nearshore plays a crucial influence on the results (de Vriend et al., 1993). In general, deep water wave information are available by either field measurements by wave buoys or hindcast by numerical models, which provide long-term time series. Thus, various techniques have been developed to define reduced synthetic wave time series representing the wave climate. The general rationale of existing methods consists in representing the wave climate as a short series of representative sea states with a given frequency of occurrence for each wave height and direction bin. The main difference between available methods lies in the approach applied to Eselect the bins and estimate the representative sea state parameters. In determining bins, wave height and direction could be grouped according to statistical clustering techniques (e.g. K-mean algorithm, Self Organizing Maps, Maximum Dissimilarity Algorithm, Camus et al., 2011b,a; Besio et al., 2017), or conservation of wave energy flux and bulk sediment transport (e.g. Walton and Dean, 1973; Steijn, 1989, 1992; Chesher and Miles, 1992; Walton and Dean, 2010; Daly et al., 2014). Benedet et al. (2016) performed a detailed comparison between different methods of wave time series reduction, including “Energy Flux method", “Energy Flux with Extreme Wave Condition Method" and “CERC Method", in which the wave height and direction bins are defined according to the concepts of equal wave energy and equal sediment transport intervals. The synthetic parameters of the representative sea state for each class are then estimated as the average values of the elements of the considered class or according to the mean wave energy flux of the class.

Moreover, each one-line model available in the literature uses its own strategy to reduce wave data in a limited number of combinations of wave height and direction. As an example, the well-known GENESIS model (Hanson, 1989) reduces the number of sea states of the whole wave time series by applying a user-defined threshold on the longshore sediment transport rate: waves inducing transport rate values higher than the threshold are grouped into a given number of wave height and direction bins to limit the computational cost of wave transformation calculations. Hence, waves inducing trasport rate values lower than the selected threshold are totally neglected. As a further example, UNIBEST-CL+ model (Deltares, 2011) simplifies wave time series in a limited number of waves by employing a probabilistic approach. The occurrence frequency of a given wave condition is used to obtain a wave time series of given duration (usually one year). As the last example, as per COVE model (Hurst et al., 2015), offshore wave parameters are synthesized by relying on the estimation of their statistical measures (i.e. mean value and standard deviation) in the whole time series.

Most of the above methods consider the whole set of offshore information to define a reduced wave time series. Nevertheless, it has to be emphasized that only sea states that induce long-term shoreline changes should be taken into account for long-term morphodynamic studies (e.g. Walton and Dean, 1973). In this respect, Walstra et al. (2013) formulated a reduction method conceived to reproduce the long-term evolution of sandy coastal stretches. Unlike other approaches, the initial time series is divided into shorter time series with a duration defined by the reduction period. The latter parameter is selected as representative of the time scale of cyclic morphological changes. The definition of the representative wave conditions is based on a weighting algorithm, which accounts for the frequency of occurrence of each wave condition in the subset. The Equivalent Wave (EW) is a further widely used method (e.g. Ciccaglione et al., 2021), based on the assumption that the equivalent wave has the same morphodynamic effects induced by the whole wave time series. The synthetic parameters of EW are usually estimated for directional sectors, chosen according to the shoreline orientation. The EW is characterized by energy flux and steepness representative of those of all waves which belong to the given directional sector. Chonwattana et al. (2005) proposed a method to reduce the offshore time series in a series of representative waves, similar to the EW concept, by taking into account the dominant sediment transport processes. Indeed, the whole time series is divided into bins of wave height and wave direction for given intervals. For each bin, the synthetic parameters of the equivalent deep water wave are estimated equating the deep water energy flux of the whole bin with that related to the equivalent sea state, for which the frequency of occurrence (e.g. its duration) is also estimated. Plecha et al. (2007) modified the method proposed by Chonwattana et al. (2005), by estimating the equivalent wave parameters at breaking for each bin, equating the energy flux at breaking of the whole bin with that of the equivalent wave. Recently, Malliouri et al. (2023) proposed a novel wave input reduction method that takes into account chronology in wave reduction techniques by using the offshore synthetic parameters of sea states only.

The reliability of the employed approach depends on the correct selection of the most representative sea states, which should induce the same long-term morphodynamic impacts as the whole wave time series. This work aims to propose a novel and easy-to-use method to define a reduced deep water wave time series starting from long historical wave time series. The proposed method may be classified as a probabilistic approach aimed to define the reduced offshore time series that induces the same long-term morphodynamic effects on sandy beaches, i.e. that has the same longshore sediment transport of the whole time series. Then, the method can be intended as an extension of the approach proposed by Plecha et al. (2007) based on the exploitation of the EW concept with the aim of providing an offshore wave time series rather than a nearshore synthetic wave climate. It has to be stressed that the proposed method allows to define the offshore reduced time series based on the long-term effects in the nearshore. It should be underlined that the chronological succession of the original wave time series is also kept. Furthermore, the method allows to preserve the uni-modal or bi-modal wave regime of the original series. One of the main strengths of the proposed method is its simplicity which is intended to not increase the computational cost of the overall long-term analyses.

The aim of this work is then threefold. First, the definition of the offshore wave time series opens the doors to the use of reliable numerical models for wave propagation nearshore (if compared to the proposed simplified method employed to reduce the time series). Second, the chronological succession is kept as it is crucial in the diagnostic reproduction of past evolution usually needed to calibrate one-line numerical models. Third, the bi-modal feature of the original time series is also kept as it can play a significant role in the shoreline response.

The paper is structured as follows. In the next Section 2, the proposed method is described in details. The results of the hydrodynamic and morphodynamic parametric analyses are illustrated in Sections 3 and 4 respectively. The findings are discussed in Section 5 that also draw some concluding remarks.

## 2. The proposed method

The proposed method aims to define a reduced offshore time series ($\mathcal{X}_e$) with the same longshore sediment transport of the offshore time series ($\mathcal{X}_w$).

If the assumption that the long-term evolution of the shoreline is driven only by the longshore component of the sediment transport applies, the reduced offshore time series $\mathcal{X}_e$ will have the same morphodynamics effect as the original wave time series (i.e. $\mathcal{X}_w$) upon the long-term evolution of the shoreline. Thus, the short-term morphodynamic effects of storm induced sediment transport acting along the transversal direction are neglected. It should be underlined that one-line models rely on the same assumptions.

The longshore component of the sediment transport can be inferred from the synthetic parameters of the given sea state (i.e. a statistical measure of the wave height, wave period, and wave angle) in its incipient breaking conditions. The widespread CERC formulation (U.S. Army Corps of Engineers, 1984) is one of the empirical tools that allow the estimation of the longshore sediment transport per unit width of the shoreline ($Q_l$):

$$Q_l = C_Q \tilde{H}_b^{5/2} \sin\left(2\tilde{\alpha}_b\right) \tag{1}$$

where $\tilde{H}_b$ is a statistical measure of the wave height at breaking and $\tilde{\alpha}_b$ is a statistical measure of the angle the wave number vector forms with the normal direction to the (local) bathymetric line. The dimensional coefficient $C_Q$ is aimed to take into account the role played by the porosity ($p$), the density ($\rho_s$) of sediments and the features of breaking waves by means of the breaker index ($\gamma$):

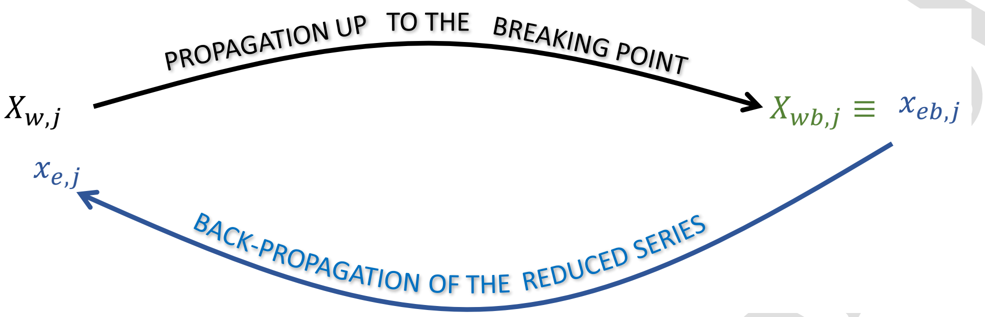


**Figure 1:** Sketch of the rationale of the proposed method.

$$C_Q = \frac{\rho g^{1/2} K}{16\gamma^{1/2}\left(\rho_s - \rho_w\right)(1-p)} \tag{2}$$

where $g$ is the gravitational acceleration and $\rho_w$ is the density of the (salt) water. The characteristic diameter of the sand grains is empirically taken into account by means of the coefficient c. it should be underlined that the value of the parameter $K$ depends also on the statistical measures selected for wave height.

Basically, the proposed method can be synthesized in the succession of the following steps (see Figure 1):

(i) propagation of each offshore sea states belonging to the $j-th$ generic subset $\mathcal{X}_{w,j}$ of the wave time series $\mathcal{X}_w$ ($\mathcal{X}_{w,j} \subset \mathcal{X}_w$), up to the breaking point in order to get the breaking wave time series $\mathcal{X}_{wb,j}$;

(ii) estimation of the total longshore sediment transport per unit width related to the sea states belonging to $\mathcal{X}_{wb,j}$;

(iii) estimation of the synthetic parameters at breaking of an equivalent sea state $\mathbf{x}_{eb,j}$ that, with a duration ($\Delta_e t$) equal to the duration of the subset $\mathcal{X}_{w,j}$, induces the same longshore sediment transport per unit width;

(iv) back-propagation offshore of the equivalent sea state to get the equivalent offshore sea state $\mathbf{x}_{e,j}$.

Hence, the (original) offshore time series $\mathcal{X}_w = \bigcup_j X_{w,j}$ is reduced to the succession $\mathcal{X}_e = \left\{\mathbf{x}_{e,1}, \mathbf{x}_{e,2}, \dots, \mathbf{x}_{e,j}, \dots\right\}$, i.e. the reduced offshore time series, both inducing the same total longshore sediment transport per unit width.

Let the wave time series $\mathcal{X}_w$ be the set of a series of chronological ordered sea states, either measured or hindcast offshore:

$$\mathcal{X}_w = \left\{\mathbf{x}_{w,1}, \dots, \mathbf{x}_{w,i}, \dots \mathbf{x}_{w,M}\right\} \tag{3}$$

where $M$ is the total number of the considered sea states and $\mathbf{x}_{w,i}$ is the offshore synthetic parameters vector of the $i-th$ generic sea state:

$$\mathbf{x}_{w,i} = \left\{ \tilde{H}_i, \tilde{T}_i, \tilde{\alpha}_i \right\} \qquad i = 1, \dots, M \tag{4}$$

where $\tilde{H}_i$ is a statistical measure of the wave height (i.e. the significant wave height, the spectral wave height, or the root mean square wave height), $\tilde{T}_i$ a statistical measure of the wave period (i.e. the peak wave period or the mean wave period) and $\tilde{\alpha}_i$ a statistical measure of the angle the wave number vector forms with the normal direction to the (local) bathymetric line (i.e. the mean wave direction).

Now, let $\mathcal{X}_{w,j}$ be a chronological ordered subset of $\mathcal{X}_w$:

$$\mathcal{X}_{w,j} = \left\{ \mathbf{x}_{w,i}, \mathbf{x}_{w,i+1}, \dots \mathbf{x}_{w,n}, \dots, \mathbf{x}_{w,i+N-1} \right\} \subset \mathcal{X}_w \tag{5}$$

where $N$ is the number of the sea states $\mathbf{x}_{w,n}$ belonging to the subset $\mathcal{X}_{w,j}$ and $\mathbf{x}_{w,i}$ is the first sea state of the subset.

In general, the propagation of each sea state can be performed by using a plethora of methods with different computational costs and reliability. It must be underlined that the method used to perform the estimation of the synthetic parameters of the sea state at the breaking conditions does not influence the method rationale, it can influence at least the reliability of the results. Due to its simplicity, the linear theory along with the Snell's law are used hereinafter. It has to be then stressed that the results should be intended as a rough approximation valid only when (i) small amplitude regular waves (with respect to both the wavelength and the water depth), (ii) mild slope, and (iii) rectilinear and parallel bathymetry assumptions apply. By intending the statistical measures $\tilde{H}_n$, $\tilde{T}_n$, and $\tilde{\alpha}_n$ (i.e. the component of the vector $\mathbf{x}_{w,n}$) as the characteristic values of a regular wave, the related (regular) breaking wave height ($\tilde{H}_{b,n}$) reads as follows:

$$\tilde{H}_{b,n} = \left( \sqrt{\frac{\gamma}{g}} \frac{\cos \tilde{\alpha}_n}{\cos \tilde{\alpha}_{b,n}} C_{g0,n} \right)^{2/5} \tilde{H}_n^{4/5} \tag{6}$$

where the wave angle at the breaking point ($\tilde{\alpha}_{b,n}$) is:

$$\tilde{\alpha}_{b,n} = \sin^{-1} \left( \sqrt{\frac{g \tilde{H}_{b,n}}{\gamma}} \frac{\sin \tilde{\alpha}_n}{C_{0,n}} \right) \tag{7}$$

with $C_{g0,n}$ the wave-group celerity that can be estimated by resorting again to the linear theory approximation taking into account the water depth at which the offshore time series is either measured or hindcast. To get the relationships

(6) and (7), the definition of the breaker index $\gamma$ ($= \tilde{H}_{b,n}/h_{b,n}$ with $h_{b,n}$ the breaking water depth; e.g. Liu et al., 2011; Lee and Cho, 2021) has been used.

Equations (6) and (7) can then be (numerically) solved in order to get the value of wave height and wave direction at breaking (i.e. $\tilde{H}_{b,n}$ and $\tilde{\alpha}_{b,n}$) needed to build the set $\mathcal{X}_{wb,j}$:

$$\mathcal{X}_{wb,j} = \left\{\mathbf{x}_{b,i}, \mathbf{x}_{b,i+1}, \ldots, \mathbf{x}_{b,n}, \ldots \mathbf{x}_{b,i+N-1}\right\} \tag{8}$$

where $\mathbf{x}_{b,n}$ is the breaking synthetic parameters vector of the $n-th$ generic sea state:

$$\mathbf{x}_{b,n} = \left\{\tilde{H}_{b,n}, \tilde{T}_n, \tilde{\alpha}_{b,n}\right\} \tag{9}$$

It should be noted that the linear assumption has been used, i.e. the wave period does not change due to the propagation.

The synthetic parameters of the equivalent sea state at breaking conditions ($\tilde{H}_{eb,j}$, $\tilde{T}_{eb,j}$, $\tilde{\alpha}_{eb,j}$) can be estimated by equating its longshore sediment transport per unit width to the average longshore sediment transport per unit width of the sea states in $\mathcal{X}_{wb,j}$, in order to obtained $\tilde{H}_{eb,j}$. It should be underlined that the rationale of the method does not depend on the formulation employed to estimate the longshore sediment transport. Hereinafter, equation (1) is used to get an analytical solution. Then:

$$\tilde{H}_{eb,j} = \left[\frac{\Delta_w t}{\Delta_e t \sin\left(2\tilde{\alpha}_{eb,j}\right)} \sum_{n=i}^{i+N-1} \tilde{H}_{b,n}^{5/2} \sin\left(2\tilde{\alpha}_{b,n}\right)\right]^{2/5} \tag{10}$$

where the direction of the equivalent sea state ($\tilde{\alpha}_{eb,j}$) is the direction of the resultant energy flux vector related to the subset $\mathcal{X}_{wb,j}$. In equation (10), the time intervals $\Delta_w t$ and $\Delta_e t$ are the temporal resolution of the original and equivalent time series respectively. It can be easily argued that $\Delta_w t < \Delta_e t$ and that $\Delta_e t = N\Delta_w t$ (i.e. the duration of the subset $\mathcal{X}_{wb,j}$).

It should be noted that the $N$ sea states in $\mathcal{X}_{wb,j}$ have been reduced to one sea state with synthetic parameters $\tilde{H}_{eb,j}$ and $\tilde{\alpha}_{eb,j}$. It could be also noted that the value of the equivalent wave period ($\tilde{T}_{eb,j}$) is not needed to estimate the equivalent wave height due to the CERC formulation (1) that does not take into account its influence on the longshore sediment transport.

The back-propagation of the equivalent sea state is performed by resorting again to the linear theory. The wave energy conservation can then be used:

$$\tilde{H}_{e,j}^2 C_{ge,j} \cos \tilde{\alpha}_{e,j} = \tilde{H}_{eb,j}^2 C_{geb,j} \cos \tilde{\alpha}_{eb,j} \tag{11}$$

where $\tilde{H}_{e,j}$ is the unknown statistical measure of the offshore wave height of the equivalent sea state, $\tilde{\alpha}_{e,j}$ and $C_{ge,j}$ are the related unknown statistical measures of the wave direction and group celerity respectively. It could be noticed that three unknowns must be evaluated.

Then, two more equations are needed. The first one is the Snell's law, and the second one is the dispersion relationship for deep water conditions at the offshore location.

An estimation of the statistical measure of the wave period of the equivalent sea state is needed. A possible definition is to equate the steepness of the offshore equivalent sea state to the average steepness of the waves belonging to the subset $\mathcal{X}_{w,j}$. Then, the wave period of the equivalent sea state reads as follows:

$$\tilde{T}_{e,j} = \sqrt{\frac{\tilde{H}_{eb,j}}{\frac{1}{N}\sum_{n=i}^{i+N-1} \tilde{H}_n / \tilde{T}_n^2}} \tag{12}$$

Equations (11) and (12) (along with the Snell's law equation and the dispersion relationship) can be solved to get the values of $\tilde{H}_{e,j}$, $\tilde{T}_{e,j}$ and $\tilde{\alpha}_{e,j}$, i.e. the offshore synthetic parameters of the sea state $\mathbf{x}_{e,j}$ that induces the same longshore sediment transport generated by the subset $\mathcal{X}_{w,j} \subset \mathcal{X}_w$:

$$\tilde{H}_{e,j} = \frac{\tilde{H}_{eb,j}}{K_R K_S} \tag{13}$$

$$\tilde{\alpha}_{e,j} = \sin^{-1}\left(\frac{C_{e,j}}{C_{eb,j}} \sin \tilde{\alpha}_{eb,j}\right) \tag{14}$$

where $K_R$ and $K_S$ are the refraction and shoaling coefficients, respectively, and $C_{e,j}$ and $C_{eb,j}$ are the offshore and at breaking wave celerity, respectively.

If the whole offshore wave time series $\mathcal{X}_w$ is divided in $N_s$ non-overlapping and consecutive subsets, the method will be applied to obtain the equivalent reduced offshore time series $\mathcal{X}_e$:

$$\mathcal{X}_e = \left\{ \mathbf{x}_{e,1}, \dots, \mathbf{x}_{e,j}, \dots, \mathbf{x}_{e,N_s} \right\} \tag{15}$$

with 172

$$\mathbf{x}_{e,j} = \left\{ \tilde{H}_{e,j}, \tilde{T}_{e,j}, \tilde{\alpha}_{e,j} \right\} \qquad j = 1, \dots, N_s \tag{16}$$

Figure 2 depicts the rationale for the offshore time series reduction. 173

It should be underlined that the equivalence is related to the net longshore sediment transport. Nevertheless, the actual evolution of the shoreline is affected by the real succession of sea states and by the related direction of the longshore sediment transport. This is particularly true when the average wave climate is bi-modal, i.e. when the direction of the longshore sediment transport is not always the same. In such cases, it is crucial to keep the bi-modal feature also in the reduced time series. 174–178

When a bi-modal wave climate is concerned, the subset $\mathcal{X}_{w,j}$ is further divided into two subsets, say them $\mathcal{X}_{w,j}^{(+)}$ and $\mathcal{X}_{w,j}^{(-)}$: 179–180

$$\mathcal{X}_{w,j} = \mathcal{X}_{w,j}^{(+)} \cup \mathcal{X}_{w,j}^{(-)} \tag{17}$$

and the proposed method remains unchanged, but the duration of the equivalent sea states, i.e. $\Delta_e t^{(+)}$ (the duration of the subset $\mathcal{X}_{w,j}^{(+)}$) and $\Delta_e t^{(-)}$ (the duration of the subset $\mathcal{X}_{w,j}^{(-)}$). In order to achieve a reduced time series equally spaced in time, a constant $\Delta_e t$ must be defined beside the actual duration of $\mathcal{X}_{w,j}^{(+)}$ and $\mathcal{X}_{w,j}^{(-)}$. It should be stressed that the invariance of the longshore sediment transport is respected thanks to equation (10) whatever the time resolution of the reduced time series, given that $\Delta_e t^{(+)} + \Delta_e t^{(-)} = N \Delta_w t$. Hence, the duration of each sea state can be defined as half of the duration of the subset $\mathcal{X}_{w,j}$, i.e. $\Delta_e t = N \Delta_w t/2$. 181–186

It should be observed that, depending on the subset $\mathcal{X}_{w,j}$, either $\mathcal{X}_{w,j}^{(+)}$ or $\mathcal{X}_{w,j}^{(-)}$ could be empty. In this case, the uni-modal version of the method can be applied to estimate the synthetic parameters of the equivalent sea state for the whole subset $\mathcal{X}_{w,j}$ that must be repeated twice (with duration $N \Delta_w t/2$) to keep a constant time resolution of the reduced time series. As a final observation, it should be noted that the number of sea states belonging to the reduced time series $\mathcal{X}_e$ for bi-modal wave climates is doubled if compared to the number of sea states belonging to reduced time series for uni-modal wave climates. 187–192

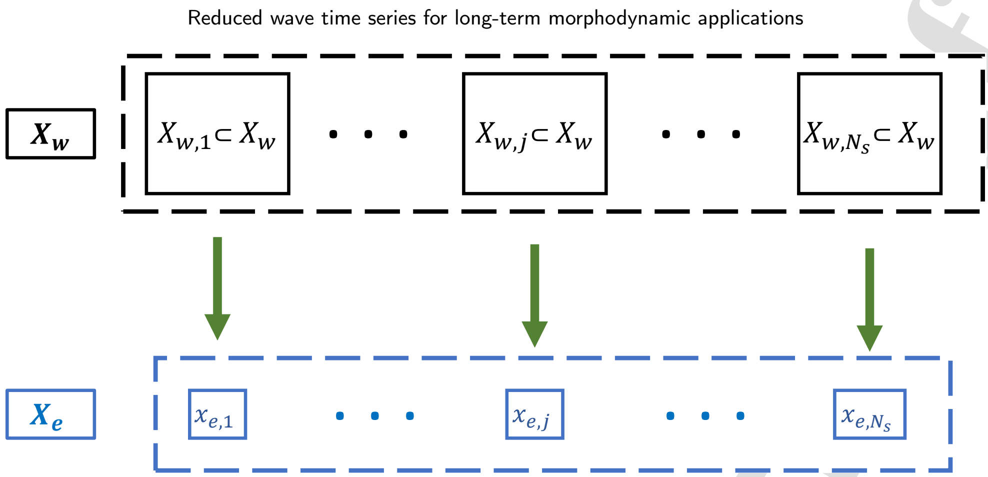


**Figure 2:** Sketch of the rationale of the offshore time series reduction.

The application of method requests the selection of a series of parameters: the number of sea states belonging to the subsets (hereinafter referred to as "block duration") and the statistical measures of the offshore synthetic wave parameters. Furthermore, it is usual to neglect the sea states with a wave height below a given threshold which can affect the results. Hence, in order to highlight the capability and reliability of the proposed method, and to gain insight into the influence of the selection of the method's parameters, a detailed parametric analysis has been performed (as illustrated in the next two sections).

## 3. Hydrodynamic parametric analysis

The hydrodynamic parametric analysis has been performed by applying the proposed method to a hindcast long-term wave series. The considered wave series has been extracted from the ERA5 reanalysis dataset provided by the European Centre for Medium-Range Weather Forecasts (ECMWF, e.g. Hersbach et al., 2020), spanning from 1950/01/01 to 2021/12/31 for a total duration of 72 years. Wave data have been extracted from a grid point (317773.89 m E, 4541018.08 m N - WGS84/UTM 33 N), located in the Tyrrhenian Sea. The extracted wave information are the significant height of combined wind waves and swell ($H_s$), the peak wave period ($T_p$), and the mean wave direction ($\alpha_m$), with a temporal resolution of one hour. Figure 3 shows the average wave climate of the selected point: it is possible to identify a prevailing offshore directional sector (W) with waves coming from different directions that cannot be neglected.

In order to apply the proposed method, the direction of the rectilinear and parallel bottom contours must be defined. Hereinafter, NW-SE oriented contours are considered, with the normal direction to the contours equal to $\theta_s = 250°$N. The reference frame illustrated in Figure 4 is then defined. The x-axis is directed along the bottom contours, hence along the shoreline. Thus, waves coming from the angular sector [250,340)°N induce negative longshore sediment fluxes (and

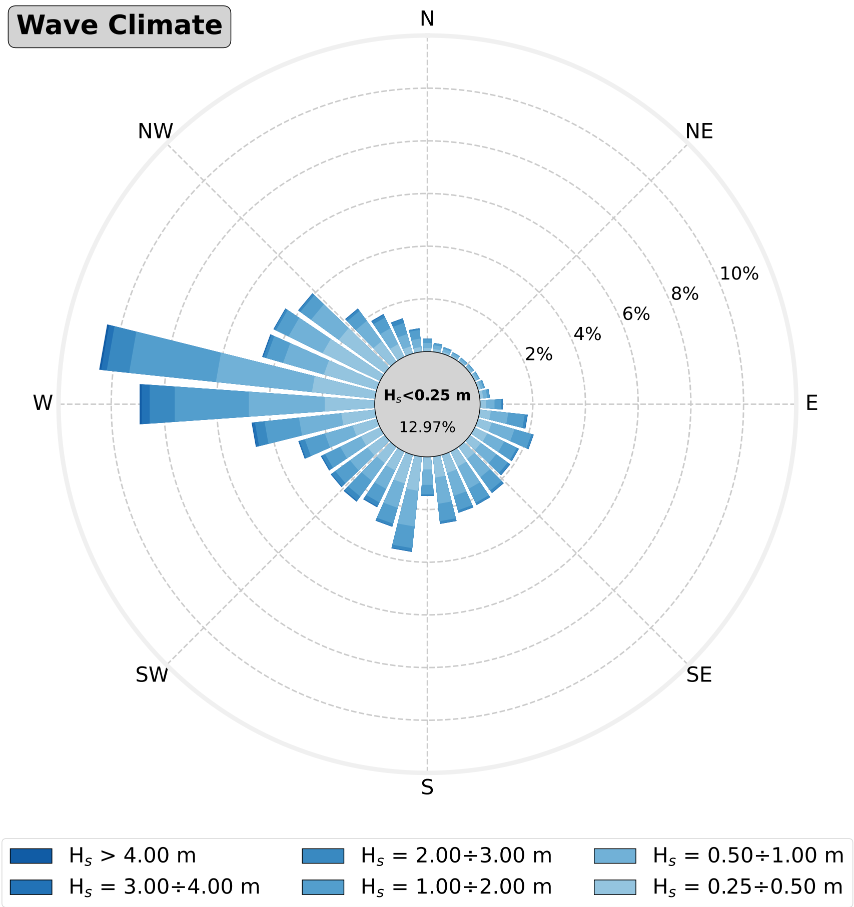


**Figure 3:** Rose diagram of the wave climate.

then negative longshore sediment transport), and waves coming from the angular sector [160,250)°N induce positive longshore sediment fluxes. As a consequence, the results of the parametric analysis illustrated in the following are related to the method applied for a bi-modal wave climate.

The parametric analysis, described hereinafter, aims to investigate the method's reliability for different selections of the method's parameters. The results obtained for the whole (i.e. original) offshore wave time series are kept as the reference test case.

In particular, the proposed method has been applied by changing the following parameters:

- duration of the blocks ($\Delta_e t$);
- threshold of the offshore wave height ($H_O^{(lim)}$, where the subscript $O$ stands for offshore conditions);

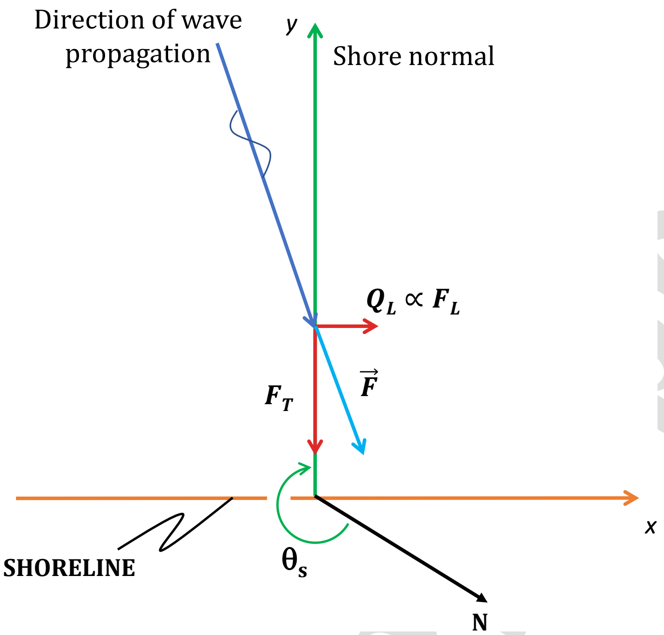


**Figure 4:** Definition sketch of shoreline orientation and positive sediment transport direction.

- threshold of the reduced breaking wave height ($H_b^{(lim)}$, where the subscript $b$ stands for breaking conditions);
- statistical measures of wave height and period (i.e. significant wave height, $H_s$, and peak period, $T_p$, vs root mean squared wave height, $H_{rms}$, and mean period, $T_m$, respectively).

First, the analysis has been carried out by comparing longshore sediment transport (net, negative and positive) induced by the whole wave series with those induced by the reduced wave series for different combinations of the parameters.

In order to gain insight into the influence of the choice of the block duration, a series of tests has been conducted by dividing the original wave series into blocks of duration $\Delta_e t$ ranging from 3 to 84 hrs, with a step of 3 hrs. The first set of tests has been performed keeping constant the values of the parameters $H_{s-O}^{(lim)}$ and $H_{s-b}^{(lim)}$, both kept equal to 0.0 m, and by using the significant wave height as the statistical measure of the wave height and the peak wave period as the statistical measure of the wave period. The mean wave direction has been taken as the statistical measure of the wave direction.

For a preliminary comparison aimed to evaluate the influence of the choice of the block duration, Figure 5 shows the duration curves of the significant wave height of the whole wave series ($\Delta_e t$ = 1 hr) and of the reduced ones (for block durations $\Delta_e t$ = 6, 12, 18, 24, 30, 36, 42, 48 hrs). Figure inspection reveals that the curves are rather close. Table 1 summarizes the numerical values of the significant wave height that is exceeded for one day in a year ($H_{1d}$), seven

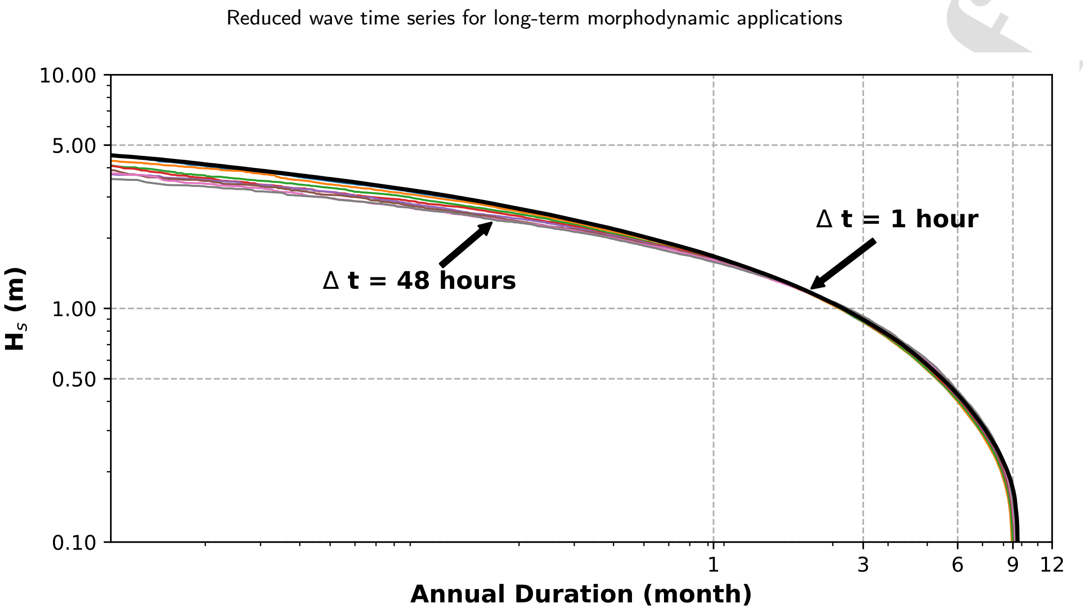


**Figure 5:** Duration curves of the significant wave height of the original and reduced wave series.

days in a year ($H_{7d}$), and $i$ months in a year ($H_{im}$, i = 1, 2, 3, 4, 5, 6, 7 and 8) for varying block duration. The lower the significant wave height duration, i.e. the larger the exceedance probability, the larger the influence of the block duration. This expected finding highlights that the longer the block duration, i.e. the larger the time step of the reduced time series ($\Delta_e t$), the lower the largest values of the significant wave height in the time series. The values of typical statistical parameters of the duration curves of the significant wave height (i.e. the wave height for duration equal to 1, 3, 6 months), remain almost unchanged for each block duration. As an example, Figure 6 shows the significant wave height exceeded one month in one year on the average ($H_{1m}$) as a function of the block duration (from 1 hr, i.e. the original wave series, up to 84 hrs). The dark grey band represents the area of $\pm5\%$ of the statistical value obtained from the original series, whilst the light grey bands represent the area of the $\pm10\%$ of the statistical value obtained from the original series. The value of $H_{1m}$ clearly decreases as the block duration increases. For block durations lower than 45 hrs, the decrease is lower than 5%.

The second group of tests has been carried out in order to investigate the role of the threshold of the offshore wave height $H_{s-O}^{(lim)}$, by keeping $H_{s-b}^{(lim)}$ equal to 0.0 m. Indeed, usually, in long-term morphodynamic applications, calm conditions are neglected, since they generate a weak longshore sediment transport ($\propto H^{5/2}$). It could be observed that this approach is implemented in GENESIS model (see section 1). Then, a threshold wave height must be defined to identify calm conditions.

**Table 1**
Statistical parameters of the duration curve of the significant wave height series as a function of the block duration ($H_{1d}$ is the value of the significant wave height that is exceeded one day in a year on the average, $H_{7d}$ is the value of the significant wave height that is exceeded seven days in a year on the average, $H_{im}$ are the values of the significant wave height that are exceeded $i$ month in a year on the average, i = 1, 2, 3, 4, 5, 6, 7 and 8).

| Block duration (hrs) | $H_{1d}$ (m) | $H_{7d}$ (m) | $H_{1m}$ (m) | $H_{2m}$ (m) | $H_{3m}$ (m) | $H_{4m}$ (m) | $H_{5m}$ (m) | $H_{6m}$ (m) | $H_{7m}$ (m) | $H_{8m}$ (m) |
|---|---|---|---|---|---|---|---|---|---|---|
| 1 | 3.95 | 2.70 | 1.68 | 1.19 | 0.91 | 0.71 | 0.56 | 0.44 | 0.34 | 0.26 |
| 6 | 3.90 | 2.67 | 1.67 | 1.18 | 0.88 | 0.69 | 0.53 | 0.41 | 0.32 | 0.24 |
| 12 | 3.83 | 2.62 | 1.64 | 1.17 | 0.88 | 0.68 | 0.53 | 0.41 | 0.31 | 0.23 |
| 18 | 3.56 | 2.56 | 1.62 | 1.18 | 0.89 | 0.69 | 0.53 | 0.41 | 0.32 | 0.24 |
| 24 | 3.46 | 2.50 | 1.64 | 1.18 | 0.90 | 0.70 | 0.54 | 0.42 | 0.33 | 0.25 |
| 30 | 3.39 | 2.43 | 1.63 | 1.19 | 0.91 | 0.71 | 0.55 | 0.43 | 0.33 | 0.25 |
| 36 | 3.38 | 2.38 | 1.62 | 1.18 | 0.92 | 0.72 | 0.56 | 0.44 | 0.34 | 0.25 |
| 42 | 3.29 | 2.36 | 1.62 | 1.17 | 0.92 | 0.72 | 0.57 | 0.44 | 0.34 | 0.26 |
| 48 | 3.23 | 2.34 | 1.59 | 1.20 | 0.93 | 0.73 | 0.59 | 0.45 | 0.36 | 0.27 |

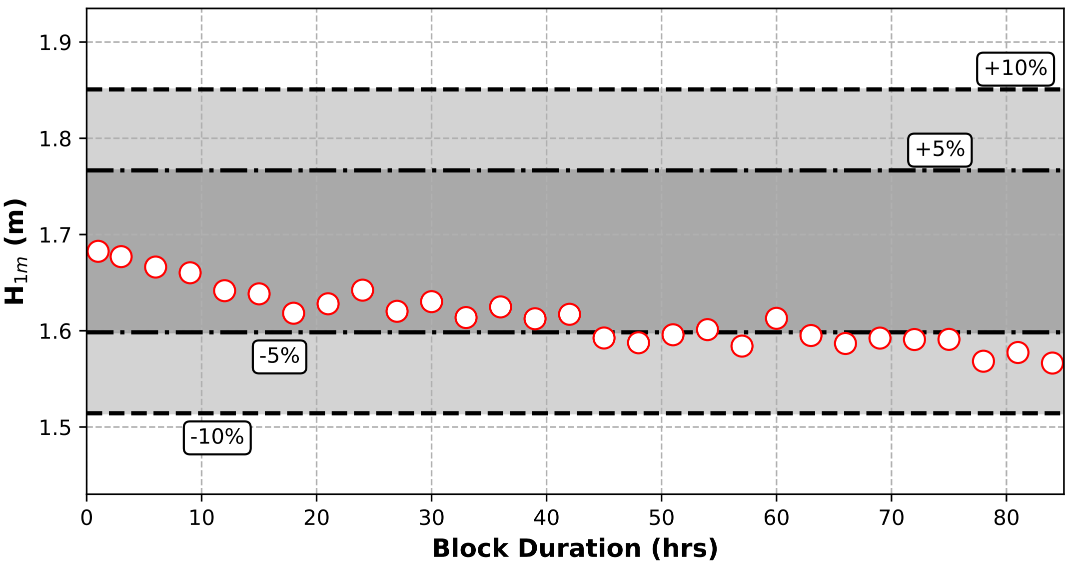


**Figure 6:** Wave height with a duration of one month ($H_{1m}$) as a function of the block duration. The shaded areas refer to the relative difference with respect to the original series (i.e. $\Delta t_e = 1$ hr).

The parameter $r$, expressed as a percentage, equal to the complement to 1 of the ratio between the total (over the investigated 72 years) longshore sediment transport induced by the reduced series and the one induced by the original wave series has been computed for the net, the positive, and the negative sediment transport for varying block duration. Figure 7 shows the results of the tests carried out setting $H^{(lim)}_{s-O}$ equal to 0.0 m (left panel), 0.25 m (middle panel) and 0.50 m (right panel). Two considerations arise from figure inspection. The results suggest a general underestimation of

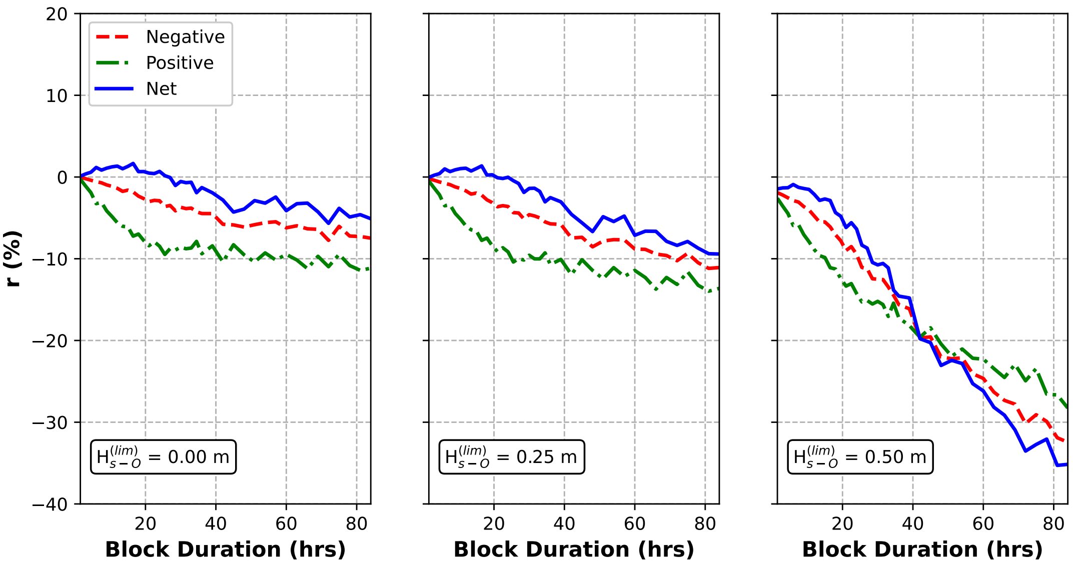


**Figure 7:** Parameter $r$, expressed as a percentage, equal to the complement to 1 of the ratio between the total (over the investigated 72 years) longshore sediment transport induced by the reduced series and the one induced by the original wave series for varying block duration and threshold of the breaking significant wave height ($H_{s-O}^{(lim)}$).

the longshore sediment transport of the reduced series: the larger the block duration, the larger the underestimation for all the tested thresholds of the offshore significant wave height. For reduced series achieved with $H_{s-O}^{(lim)} = 0.00$ m, the sediment transport maximum underestimation is roughly equal to 5%, 7% and 10% for the net, negative and positive sediment transport respectively. As the threshold of the offshore significant wave height increases, the underestimation increases too. For $H_{s-O}^{(lim)} = 0.25$ m the maximum underestimation slightly increases with respect the threshold equal to 0.00 m. Nevertheless, the results obtained for $H_{s-O}^{(lim)} = 0.50$ m reveal that the maximum underestimation dramatically increases up to roughly 30%. On the one hand, it should be stressed that this finding is site dependent (in this case the percentage of wave with significant wave height $H_{s-O} < 0.50$ m is equal to 40.6%) as it is heavily influenced by the duration curve of the significant wave height (e.g. Figure 5). On the other hand, it highlights the needing to investigate the role of the threshold to be used to get reliable results (with respect to the whole wave time series).

A similar comparison has been made for the threshold $H_{s-b}^{(lim)}$, by keeping $H_{s-O}^{(lim)}$ equal to 0.0 m. Figure 8 shows the obtained results, for $H_{s-b}^{(lim)}$ equal to 0.0 m (left panel), 0.25 m (middle panel) and 0.50 m (right panel). The sediment transport underestimation increases as the block duration and the threshold $H_{s-b}^{(lim)}$ increase. From a quantitative point of view, similar values as discussed for the offshore threshold of the offshore significant wave height are obtained.

Furthermore, the proposed method has been applied by using root mean square wave height ($\tilde{H}_i = H_{rms}$) and mean period ($\tilde{T}_i = T_m$) as the statistical measure of the offshore wave parameters. By assuming that the individual

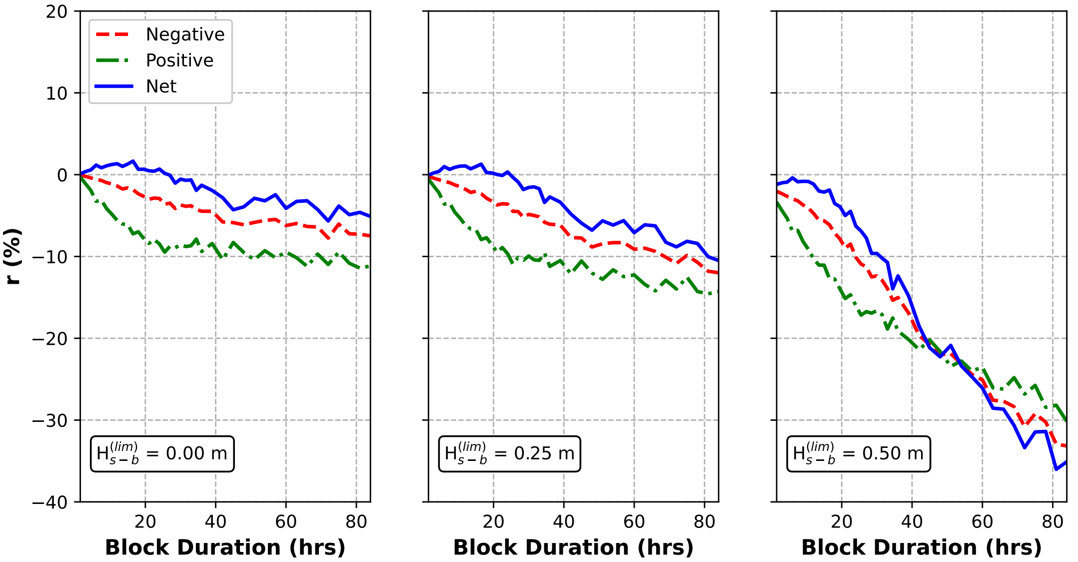


**Figure 8:** Parameter $r$, expressed as a percentage, equal to the complement to 1 of the ratio between the total (over the investigated 72 years) longshore sediment transport induced by the reduced series and the one induced by the original wave series for varying block duration and threshold of the breaking significant wave height ($H^{(lim)}_{s-b}$).

wave height belongs to the population of a stochastic variable with a Rayleigh Cumulative Distribution Function (e.g. Battjes and Groenendijk, 2000; Celli et al., 2018), the following relationships apply:

$$H_{rms} = \frac{H_s}{\sqrt{2}} \qquad T_m = \frac{T_p}{1.2} \tag{18}$$

The use of the root mean squared wave height requests a discussion on the computation of sediment transport. Indeed, the CERC formula (U.S. Army Corps of Engineers, 1984) can be applied by using both significant and root mean square wave height at breaking by changing the value of the parameter $K$ (equal to 0.39 and 0.77 for significant and root mean squared wave height respectively).

The parameter $r$, expressed as a percentage, equal to the complement to 1 of the ratio between the longshore sediment components induced by the wave series of $H_{rms}$ and $T_m$, and those induced by the original wave series of $H_s$ and $T_p$ has been evaluated. The thresholds $H^{(lim)}_{rms-O}$ and $H^{(lim)}_{rms-b}$ are both set equal to 0.00 m. Figure 9 shows the obtained results. It can be noted, also in these cases, that the parameter $r$ decreases as the duration of the block increases. Differently from the results of Figures 7 and 8, $r$ assumes negative values of about 17% already for small block durations, up to values greater than 20% for block duration of 84 hrs. This result is related to the different

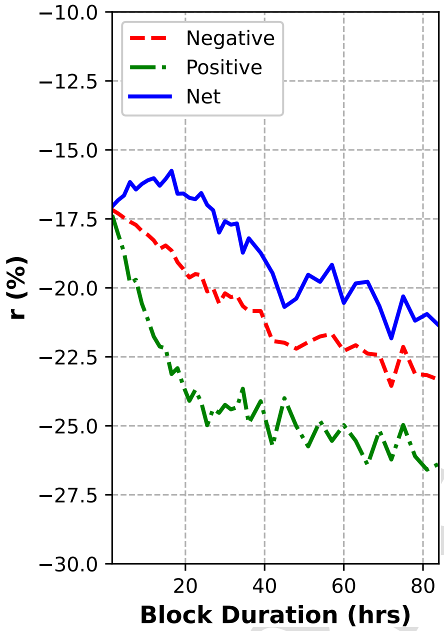


**Figure 9:** Parameter $r$, expressed as a percentage, equal to the complement to 1 of the ratio between the longshore sediment components induced by the wave series of $H_{rms}$ and $T_m$, for varying block duration, and those induced by the original wave series of $H_s$ and $T_p$.

definition of the ratio $r$ that is defined with respect to the results obtained with the original wave time series of the significant wave height that is not totally recovered by the increased value of the $K$ parameter in the CERC formula due to the different propagation results (performed with $T_m$ instead of $T_p$).

A further investigation has been carried out by comparing the cross-shore distribution of energy dissipation due to breaking waves. For this purpose, the whole original and the reduced wave series (obtained keeping $H_{s-O}^{(lim)}$ and $H_{s-b}^{(lim)}$ equal to 0.0 m) have been propagated inshore along an ideal Dean profile ($h = Ay^{2/3}$ with $h$ the water depth, $y$ the cross-shore distance and $A$ the shape parameter, e.g. Dean, 1977) defined by setting the parameter $A = 0.01$. The wave propagation up to the shoreline location has been performed by using the wave transformation model proposed by Dally et al. (1985). Then, the dissipation rate due to wave breaking has been estimated using the formula proposed by Battjes and Janssen (1978):

$$D_b = \frac{\alpha}{4} Q_b f \rho_w g H_m^2 \tag{19}$$

where $\alpha$ is a constant ($\simeq 1$); $\rho_w$ is the seawater density; $g$ is the gravitational acceleration; $f$ is the representative frequency of the energy spectrum ($= 1/\tilde{T}_i$); $H_m$ is the maximum possible wave height for breaking or broken waves and

it can be calculated applying one of the breaking criterion presented in literature (e.g. Liu et al., 2011). The parameter 299
$Q_b$ represents the fraction of broken waves that can be estimated as follows (e.g. Battjes and Janssen, 1978): 300

$$\frac{1 - Q_b}{\ln Q_b} = -\left(\frac{H_{rms}}{H_m}\right)^2 \tag{20}$$

In the upper panel of Figure 10, the dimensionless dissipation functions $D^* (= D/D_{max})$, given by the superposition 301
of dissipation rate of all the considered sea states ($D$) normalized by its maximum value ($D_{max}$) dissipation of the 302
wave series, is represented as a function of the water depth $h$. The original wave series with a time resolution of 1 hr 303
is described by a solid line, the reduced ones, with block duration ranging between 3 to 45 hrs with 3 hrs step, are 304
represented by solid grey lines, and the reduced wave series with block duration equal to 48 hrs is represented by the 305
dashed line. It is possible to realize that the normalized dissipation function moves towards the shore as the block 306
duration increases, due to the lower values of the significant wave height $H_s$ of the reduced series (in according with 307
results of Table 1). In the lower panel of Figure 10, the width of the surf zone (defined as the distance from the shore 308
where $D^*$ is greater than a given value $D_{min}$) is shown for each reduced wave series: the larger the block duration the 309
narrower the surf zone. This result is consistent with the discussion of the duration curve of the significant wave height: 310
the longer the block duration, the lower the largest values of the significant wave height in the time series, and then the 311
lower the water depth where the breaking processes start to occur. 312

The shaded area refers to the water depth interval between the annual and decennial closure depths, estimated by 313
applying Hallermeier's formula (Hallermeier, 1978, 1980) as approximated by CUR (1987): 314

$$DoC = 1.6 H_{s_{12h}} \tag{21}$$

where $H_{s_{12h}}$ is the significant wave height which occurs 12 hrs during the considered time interval (either one year 315
– annual closure depth – or ten years – decennial closure depth) on average. Figure 10 inspection reveals that the 316
estimated long-term surf zone width is roughly consistent with the long-term active coastal zone width. 317

## 4. Morphodynamic parametric analysis 318

This section aims to address the influence of the block duration upon the (numerically simulated) evolution of an 319
ideal sandy beach under the action of waves. Both the long- and short-term evolution of the shoreline have been then 320
investigated. 321

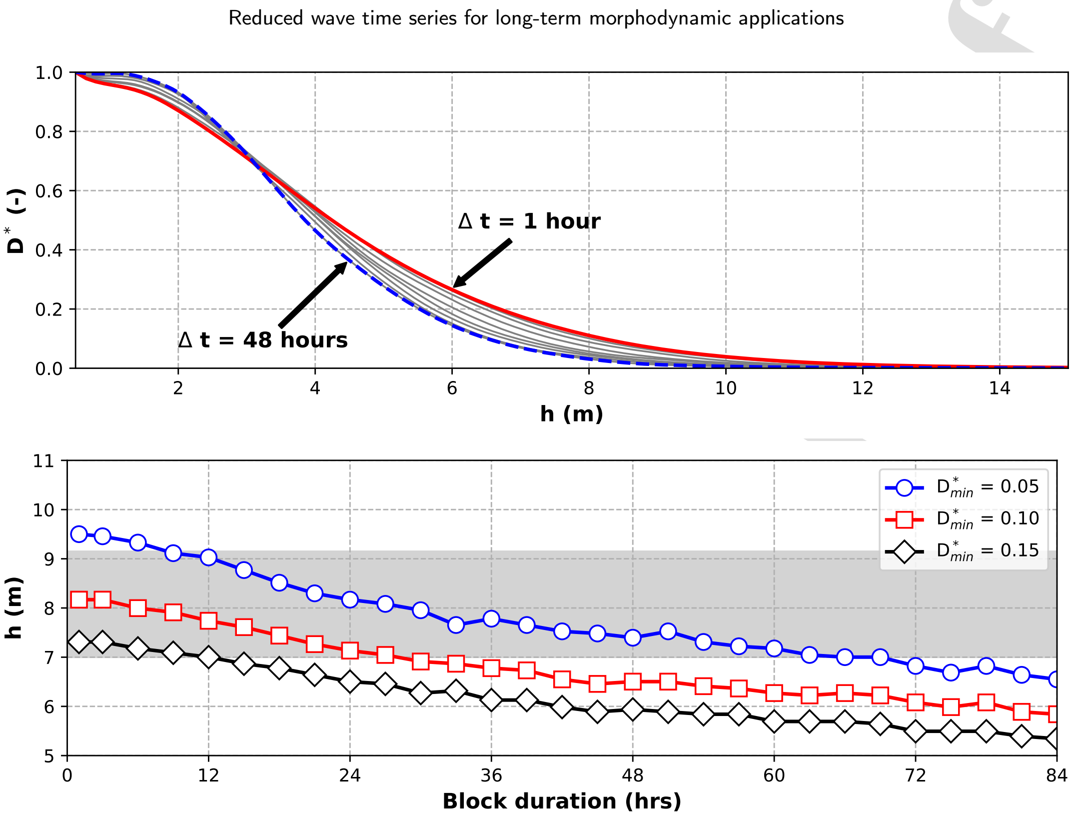


**Figure 10:** Comparison of dissipation function shape between the original and the reduced wave series (upper panel) and estimated long-term extension of the surf zone (lower panel). The shaded area refers to the water depth interval between the estimated annual and decennial closure depths.

As far as the long-term evolution is concerned, the one-line modeling approach has been applied. The used numerical model has been implemented to reproduce the long-term morphodynamic evolution of sandy beaches in response to gradients in longshore sediment transport, generated by breaking waves. The model is based on the well-known Pelnard-Considére's assumption that the cross-shore beach profile shape (average profile) remains constant in the long-term (e.g. Pelnard-Considére, 1956). Hence, it is allowed to translate along the normal direction to the shore. The beach profile extends offshore up to the depth of closure, where there is no significant sand transport (e.g. Hallermeier, 1978, 1980). The governing equation for the simplified problem is then the conservation of the sediment mass:

$$\frac{\partial y_L}{\partial t} = -\frac{1}{DoC + D_B}\left(\frac{\partial Q_l}{\partial x} \pm q\right) \tag{22}$$

where $y_L$ represents the position of the long-term shoreline, $t$ is the time, $DoC$ is the depth of closure, $D_B$ is the berm height, $x$ represents the axis parallel to the average direction of shoreline, $Q_l$ is the longshore sediment transport rate and $q$ empirically accounts for gains or losses of sand, per unit width, in the cross-shore direction (i.e. due to river sediment transport, losses related to rip currents, beach nourishment, sand by-passing, etc...).

The longshore sand transport $Q_l$ has been estimated by using the CERC (U.S. Army Corps of Engineers, 1984) formula (see Equation 1). The synthetic parameters of breaking waves are evaluated by means of the method proposed by Dally et al. (1985). The governing Equation (22) is numerically solved by using Runge Kutta 4th-order method. The longshore gradient of the sediment transport is approximated by a centered first-order scheme applied on a staggered grid.

The model has been validated by means of comparison with the analytical solutions, proposed by Larson et al. (1987), for different shoreline configurations (e.g. Scipione, 2022). Since shoreline evolution models have a significant role in the planning process and optimization of coastal area restoration, the proposed model allows to reproduce the morphodynamic impacts of coastal defense measures, such as groynes and nourishment, usually used to protect and stabilize beaches against erosion (e.g. Di Risio et al., 2010).

The model is also capable to simulate shoreline response to transversal coastal structures (i.e. groynes) by means of a non-linear time-dependent bypassing coefficient. Indeed, groynes act on the longshore sediment transport by trapping it partially or totally, depending on the effective length ($L_{eff}$) of the groyne, i.e. depending on the distance between the offshore tip of the structure and the (instantaneous) long-term location of the shoreline. Since the long-term shoreline location ($y_L$) varies in time, also $L_{eff}$ varies in time. In order to estimate the trapping efficiency of groynes, the longshore sediment transport distribution along the transversal direction must be known. Thus, the cross-shore distribution of the longshore sediment transport inside the surf zone has been assumed proportional to the dimensionless wave-breaking dissipation function $D$ given by equation (19), which varies with the propagated sea state (e.g. Bagnold, 1963; Bailard and Inman, 1981; Bodge, 1989; Smith and Wang, 2002; Baykal et al., 2012; Goda, 2013). Then, groynes' effects on the long-term evolution of the shoreline, i.e. the longshore sediment transport $Q_g$ at the groyne location, can be described by applying a bypass coefficient ($\xi_g$) to the longshore sediment transport evaluated by means of the CERC formula updrift the groyne ($Q_l^{(u)}$):

$$Q_g = \xi_g Q_l^{(u)} \tag{23}$$

where the bypass coefficient, which accounts for sand bypassing around the offshore tip of the groyne, can be defined as follows:

$$\xi_g(t) = 1 - \frac{\int_0^{L_{eff}(t)} D dy}{\int_0^{y^*} D dy} \tag{24}$$

where $y^*$ is the offshore limit of the surf zone. 358

The bypass coefficient $\xi_g(t)$ is a function of $L_{eff}(t)$ and of the cross-shore distribution of the longshore sand transport that depends on the instantaneous sea state.

The model has been applied to an ideal sandy pocket beach. The initial shoreline is rectilinear, directed along the x-axis. At the lateral boundaries, the longshore sediment transport is imposed to be zero. The simulated period is equal to one year. The extension of the numerical domain along the x-axis has been set to 3000 m.

Four case studies have been considered: the long-term evolution of the shoreline without any structure (referred to as "free long-term evolution" hereinafter); the long-term evolution of the shoreline influenced by a groyne deployed at the center of the numerical domain with different lengths (referred to as "long-term evolution with groyne" hereinafter). Indeed, the influence of the groyne configuration has been investigated by simulating three different groyne lengths: 50 m (referred to as "short groyne" hereinafter), 250 m (referred to as "medium groyne" hereinafter), and 500 m (referred to as "long groyne" hereinafter). The governing equation has been then integrated with a time step equal to 10 minutes. The spatial derivative (of the longshore sediment transport) has been evaluated with a uniform spatial discretization equal to 25 m.

Figure 11 shows the numerical results in terms of the average and final configuration of the computed long-term shoreline (left panels) and of the Interquartile Range (hereinafter referred to as $IQR_L$) of the long-term shoreline evolution (right panels). The results are reported for the original wave series ($\Delta_e t = 1$ hr) and for the reduced series for $\Delta_e t$=[6,84] hrs (by using the significant wave height as the statistical measure of the wave height, the peak wave period as the statistical measure of the wave period, and with thresholds of offshore and breaking significant wave height set to zero). In the upper panels, the results obtained for the free evolution test case are shown. In the lower panels, from top to down, the results obtained for short, medium, and long groyne are reported.

First, the long-term free shoreline evolution is commented on. It can be observed that the net sediment transport is negative, consistently with the wave climate (see Figure 3). Then, the shoreline rotates clockwise. The block duration influence is rather clear: the larger the block duration, the lower the shoreline displacement (for both the mean shoreline and its final configuration). This is consistent with the increase of the underestimation of longshore sediment transport for increasing block duration (Figure 7, Section 3). Table 2 synthesizes the obtained numerical results. For the longest tested block duration (84 hrs), the underestimation of the shoreline displacement at the boundary of the numerical domain reaches about 19.0 m and 15.0 m for the averaged and final configurations, respectively. The analysis of the

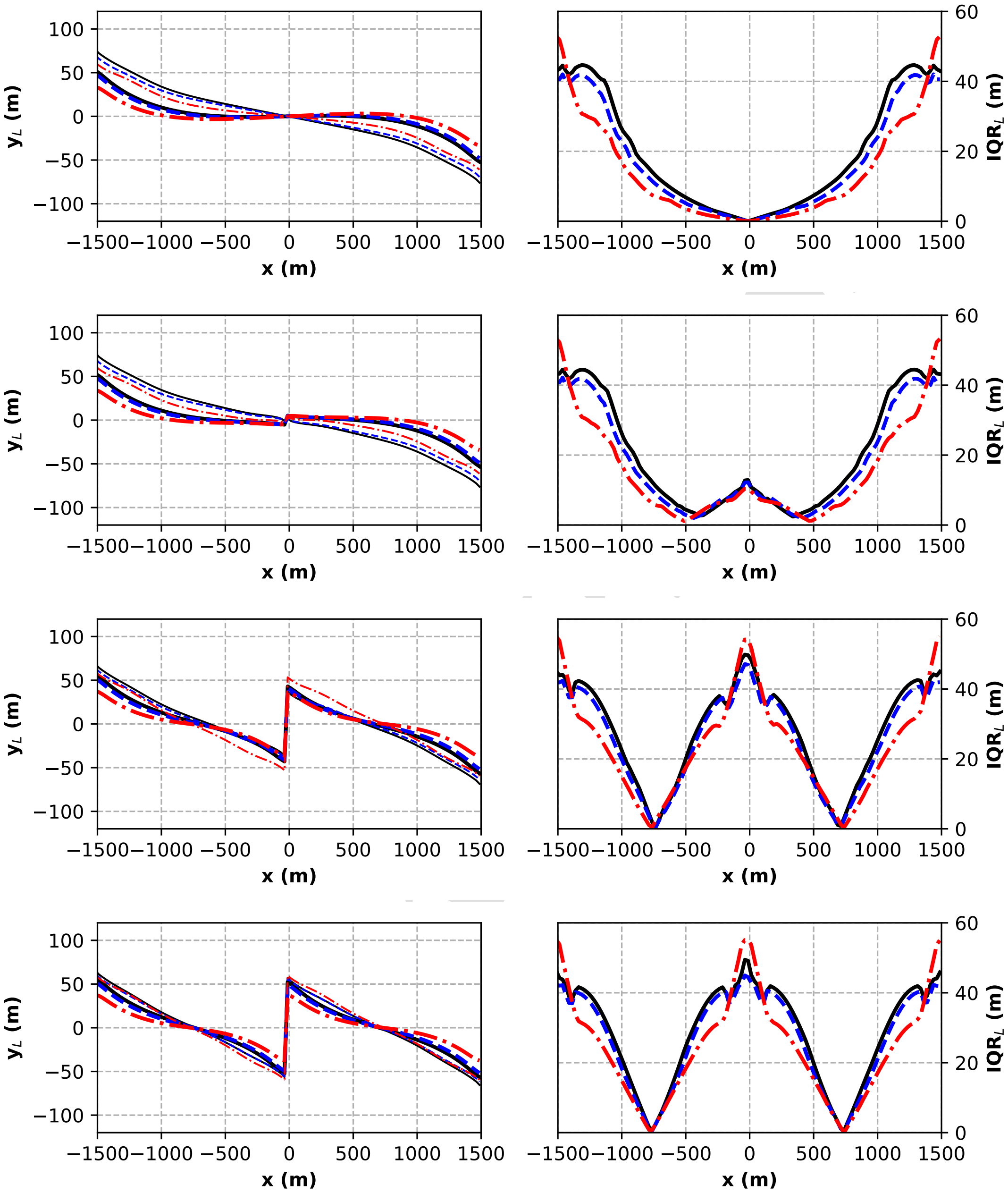


**Figure 11:** Computed long-term evolution of the shoreline. Left panels: average (thick lines) and final (thin lines) configuration of the shoreline. Right panels: Interquartile Range ($IQR_L$) of the shoreline evolution. In each panel, the results obtained for block duration equal to 1 hr (continuous lines), 6 hrs (dashed lines), and 84 hrs (dot-dashed lines) are shown.

statistical measure of the shoreline displacement over time is meaningful (i.e. the Interquartile Range, Figure 11, upper panel on the right). Indeed, the center of rotation ($IQR_L = 0$) is the same for all the tested block duration, as expected (due to the symmetry of the domain and the numerical scheme). In general, the larger the block duration, the lower the variation of the shoreline. This is not the case directly close to the boundaries of the domain where the longest tested block duration is related to a larger variation of the shoreline location.

When the long-term effect of groynes is concerned, the interpretation of the obtained results seems to be less obvious (see numerical results in Table 3). Negligible differences with respect to the long-term free evolution are observed in terms of the influence of the block duration: the maximum underestimation is again equal to about 19.0 m. Nevertheless, the underestimation seems to decrease for increasing block duration if the final configuration of the shoreline is considered. To shed light on this anomalous features of the results, the shoreline just updrift the groyne (i.e. $x = x_G^+$) has been sampled and analyzed. In this case, an overestimation is observed if the final configuration of the shoreline is considered. The overestimation is small (at least negligible) for the shortest (i.e. 50 m) and longest (i.e. 500 m) groyne lengths. The largest overestimation (i.e. +16.1 m) is observed for the medium groyne (i.e. 250 m long). The obtained results can be interpreted by the trapping efficiency of the groyne and to the results of the parametric analysis in terms of the curve duration of the significant wave height. Indeed, for the short and long groyne, it can be argued that the trapping efficiency is not significantly affected by the block duration. For short groyne, only the longshore sediment transport induced by sea state with low energy are totally trapped. For long groyne, the longshore sediment transport induced by almost all the sea states is trapped. For the medium groyne, the sediment transport induced by large significant wave heights is not totally trapped. As the larger the block duration, the lower the highest value of significant wave height (in the time series), the narrower the surf zone width (Figure 10, section 3) and then the larger the trapping efficiency of the groyne. The influence of the surf zone width with respect to the groyne length upon its trapping efficiency is a key to understanding also the decrease of the underestimation at the boundary of the domain: the longshore sediment transport underestimation (Figure 7, Section 3) is balanced by the variation of the trapping efficiency of the groyne and by the decreased distance to the boundary of the "centre of rotation" ($IQR_L \simeq 0$ in right panels of Figure 11) of the shoreline.

As far as the short-term evolution is concerned, the model proposed by Yates et al. (2009) has been applied for wave series with varying block duration. They argued that the short-term evolution of the shoreline location ($y_s$) is influenced by the instantaneous difference between the incoming wave energy ($E_w$) and a kind of equilibrium energy ($E_{eq}$):

$$\frac{\partial y_s}{\partial t} = -CE^{1/2}\left(E_w - E_{eq}\right) \tag{25}$$

**Table 2**
Summary of the numerical results in terms of the free long-term evolution of the shoreline. The long-term location of the shoreline, $y_L(x,t)$ is sampled at the boundary of the domain ($x = 0$) and averaged over the whole simulation (the overbar symbol indicates the averaged values). The final values are also reported ($t = t_{end}$). The symbol $\Delta$ indicate the difference with respect the original wave series (i.e. duration equal to 1 hr). The speed up of the simulation is reported as well.

| | Free long-term evolution | | |
|---|---|---|---|
| Block duration (hrs) | 1 | 6 | 84 |
| $\overline{y_L(x=0,t)}$ (m) | 52.0 | 47.9 | 33.4 |
| $\Delta \overline{y_L(x=0,t)}$ (m) | = | −4.1 | −18.6 |
| $y_L(x=0,t_{end})$ (m) | 75.9 | 69.3 | 61.0 |
| $\Delta y_L(x=0,t_{end})$ (m) | = | −6.6 | −14.9 |
| Speed up (-) | = | 5.4 | 27.2 |

**Table 3**
Summary of the numerical results in terms of the long-term evolution of the shoreline when a groyne is deployed at the centre of the domain ($x_G$). The superscript in $x_G^+$ indicates the updrift side of the groyne. See caption of Table 2 for other symbols.

| | Short Groyne | | | Medium Groyne | | | Long Groyne | | |
|---|---|---|---|---|---|---|---|---|---|
| Block duration (hrs) | 1 | 6 | 84 | 1 | 6 | 84 | 1 | 6 | 84 |
| $\overline{y_L(x=0,t)}$ (m) | 53.0 | 48.8 | 34.3 | 56.6 | 51.7 | 37.4 | 56.5 | 51.8 | 37.7 |
| $\Delta \overline{y_L(x=0,t)}$ (m) | = | −4.2 | −18.7 | = | −4.9 | −19.1 | = | −4.8 | −18.8 |
| $y_L(x=0,t_{end})$ (m) | 76.2 | 69.5 | 61.2 | 68.0 | 63.5 | 59.1 | 64.8 | 61.2 | 59.2 |
| $\Delta y_L(x=0,t_{end})$ (m) | = | −6.7 | −15.0 | = | −4.6 | −6.7 | = | −3.6 | −5.6 |
| $\overline{y_L(x=x_G^+,t)}$ (m) | 5.1 | 5.0 | 4.4 | 43.0 | 41.0 | 36.2 | 52.5 | 49.5 | 37.4 |
| $\Delta \overline{y_L(x=x_G^+,t)}$ (m) | = | −0.1 | −0.7 | = | −2.0 | −6.8 | = | −3.0 | −15.1 |
| $y_L(x=x_G^+,t_{end})$ (m) | 1.6 | 1.8 | 2.9 | 37.2 | 39.1 | 53.3 | 57.1 | 56.4 | 59.6 |
| $\Delta y_L(x=x_G^+,t_{end})$ (m) | = | +0.2 | +1.3 | = | +1.9 | +16.1 | = | −0.7 | +2.4 |
| Speed up (-) | = | 5.1 | 20.5 | = | 5.1 | 20.7 | = | 5.1 | 20.7 |

where $C$ is the change rate coefficient for both short term accretion ($E_w < E_{eq}$) and erosion ($E_w > E_{eq}$), as suggested by Vitousek et al. (2017) and Long and Plant (2012).

The (measure of the) instantaneous wave energy ($E_w$) has been defined as the wave height squared (Yates et al., 2009; Vitousek et al., 2017).

The equilibrium wave energy ($E_{eq}$) is related to the instantaneous short-term location of the shoreline. An empirical relationship for the equilibrium wave energy has been proposed by Yates et al. (2009):

$$E_{eq} = a y_s + b \tag{26}$$

where $a$ and $b$ are two empirical parameters of the model.

From a physical point of view, equations (25) and (26) state that an equilibrium wave energy exists for a given location of the short-term location of the shoreline.

The model proposed by Yates et al. (2009) has been applied to investigate the role of the block duration upon the short-term evolution of the shoreline location. Then, equation (25) has been integrated by Runge-Kutta 4th order method with a time step equal to 10 minutes. Typical values of the parameters $C$, $a$ and $b$ have been considered, equal to 0.1 (m/m$^3$/day), $-0.05$ (m$^2$/m) and 0.5 (m$^2$) respectively (e.g. Vitousek et al., 2017).

The initial condition is set to $y_s(0) = 0$.

Figure 12 shows the obtained results in terms of time series of the short-term location of the shoreline. As underlined by Yates et al. (2009), the transient effects of the unbalanced wave energy (i.e. $E_w \neq E_{eq}$) is superposed to the long-term location of the short-term shoreline ($y_{s-eq}$). Hence, the mean value of the computed short-term shoreline (i.e. $y_{s-eq}$) has been removed from the time series shown in Figure 12. As expected, the short-term location of the shoreline is characterized by advances and retreats. Nevertheless, the amplitude of the oscillations decreases as the block duration increases (Figure 12, lower panels). Again, this is related to the influence of the block duration upon the duration curve of the significant wave height: the larger the block duration, the lower the highest value of significant wave height (in the time series), the lower the incoming wave energy (see $E_w$ in Figure 12), the lower the short-term displacement of the shoreline.

## 5. Discussion and concluding remarks

The proposed method allows to define the (reduced) offshore wave time series that has the same effects upon the long-term evolution of the original wave time series.

In particular, the method allows to preserve the chronological order of the whole time series and the dominant wave directions of the original wave series. Both aspects, that are not always considered in previous methods (e.g. Chonwattana et al., 2005; Plecha et al., 2007; Benedet et al., 2016), are recognized to play a crucial role in the long-term response of the shoreline of sandy beaches (e.g. Southgate, 1995; Walstra et al., 2013; Antolínez et al., 2016). On one hand, the correct sequence of the reduced wave time series can be meaningful within the frame of numerical model calibration. Indeed, the use of one-line models relies on the correct selection of the models' parameters. Usually, this selection is based on the comparison of observed long-term shoreline evolution against the estimated one. Then, the use of a representative wave time series with the appropriate time sequence may be of great interest for numerical modelers. Of course, the chronological order can be synthesized only for diagnostic studies, e.g. only for numerical simulations aimed to reproduce past long-term evolution. Nevertheless, the method can be further used to define representative offshore wave time series to estimate future long-term evolution. Indeed, the reduced offshore time series can be used

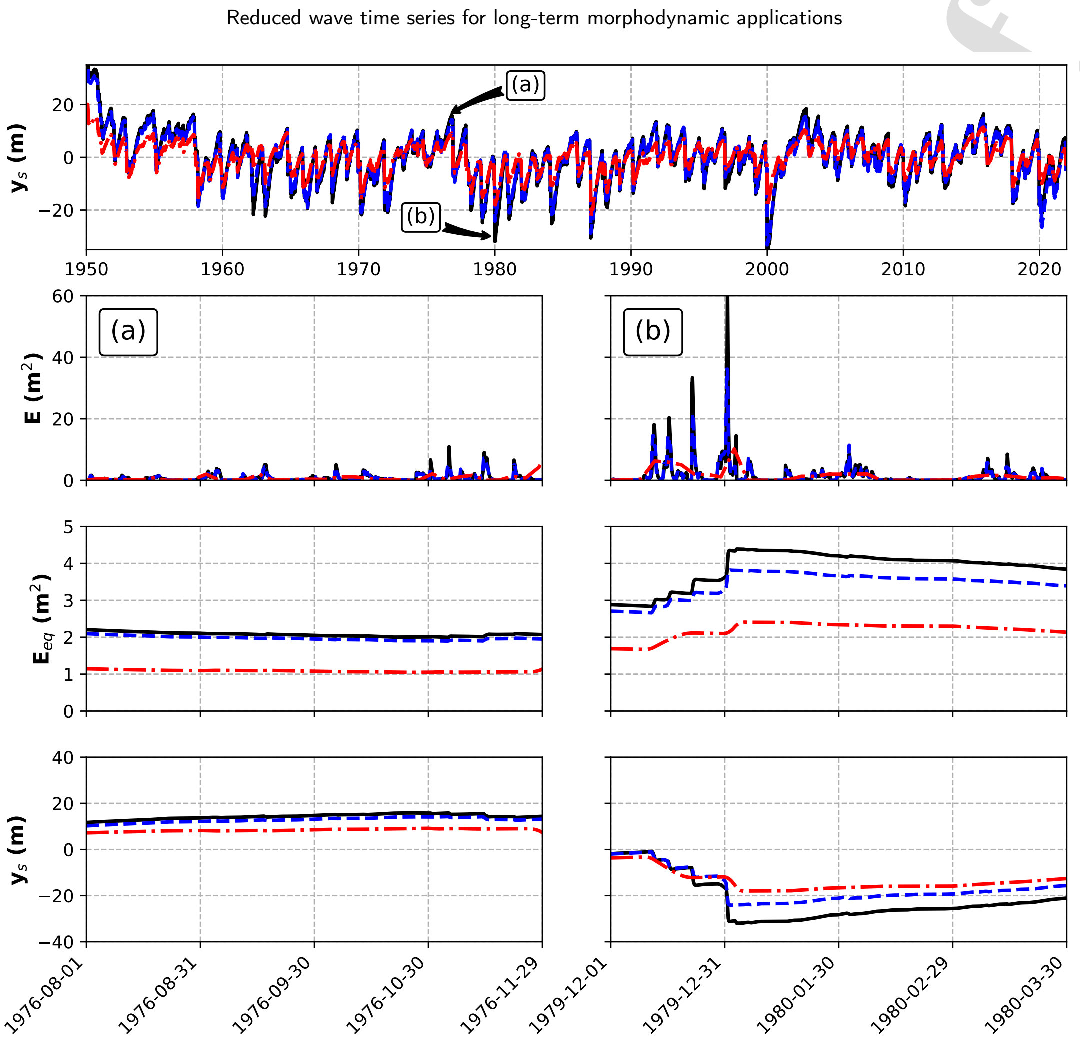


**Figure 12:** Computed short-term evolution of the shoreline. In each panel, the results obtained for block duration equal to 1 hr (continuous lines), 6 hrs (dashed lines) and 84 hrs (dot-dashed lines) are shown.

as input data to methods available in the literature to synthesize reliable (future) series with appropriate time sequence (e.g. Southgate, 1995; Walstra et al., 2013; Antolínez et al., 2016).

Furthermore, the correct reproduction of the approaching wave climate is necessary to get a reliable reproduction and prediction of the long-term beach response (e.g. Daly et al., 2014). Indeed, the bi-modal features of certain wave climates, correctly reproduced by the proposed method, influence the long-term morphodynamic response of the beach in terms of longshore sediment transport direction, thus of distribution of sediment along the stretch and, finally, of shoreline orientation (e.g. Pelnard-Considére, 1956).

The proposed method relies on a series of simplifications in order to make it both reliable and easy-to-use for practical applications by professionals. In particular, the linear theory is used to propagate the (original) wave series up to the breaking point and, then, to perform the back-propagation offshore of the (reduced) wave series (Figure 1). Nevertheless, the back-propagation step allows to use accurate wave propagation methods at the modeling stage. Indeed, the simplification of the reduction method can be removed when actual morphodynamics simulations are performed. This observation highlights the needing to have the reduced wave series at the offshore boundary of the area of interest instead of the breaking wave time series. A further simplification of the proposed method is related to the use of the CERC formula (e.g. U.S. Army Corps of Engineers, 1984) to perform the parametric analysis aimed to investigate the reliability approach (Sections 3-4). However, it should be underlined that the method is flexible and other formulations for the estimation of the longshore sediment transport can be used as well (e.g. Kamphuis, 1991). Further simplifications of the proposed approach are inherited from the one-line model assumptions, intimately related to the aim of the analysis to assess the long-term evolution of shorelines, hence by neglecting the phenomena taking place in the short-term (i.e., related to the temporal scale of storms). Indeed, the long-term evolution is assumed to be driven by longshore sediment-transport gradients, while the cross-shore sediment transport is neglected. The latter assumption means that the cross-shore profile remains unchanged and is given as a mean profile (e.g. Dean, 1977). In other words, the effects of storm-induced phenomena are not taken into account (i.e., the influence of breaking bars). It could be observed that severe storms will produce important variations in the long-term shoreline evolution if sediment losses occur. Nevertheless, such kind of short-term phenomena influencing long-term evolution can be taken into account in the mass conservation equation solved by one-line models by including sediment losses (e.g. storm bypassing). Furthermore, the effects of short-term variation of sea level (i.e. tides, wave set-down, wave set-up, etc...) are not included in the method. These aspects are further discussed in the following.

The parametric analysis (see Sections 3-4) revealed that the larger the block duration of the reduced time series, i.e. the lower the number of sea states belonging to the series (and then the lower the computational cost of morphodynamic simulations), the lower the highest value of the significant wave height. As expected, the increase of block duration gets worse the capability of the reduced series to represent the storms, i.e. the most energetic sea state in the original time series. On the one hand, this aspect could be important if the short-term evolution has to be reproduced (e.g. Figure 12) or if the long-term trapping efficiency of groynes, related to the width of surf zone, has to be taken into account (e.g. Figure 11). On the other hand, the long-term evolution and the induced longshore sediment transport are still well reproduced for large block duration (e.g. Figure 7), at least within the typical accuracy of one-line models. The parametric analysis served also to investigate the role of the selection of the statistical measures of synthetic parameters of sea states. This selection does not significantly influence the reliability of the method. Rather, the calibration coefficients (e.g. parameter $K$ of the CERC formula) can mitigate the unreliability mainly related to the methods employed for propagation, and back-propagation as well.

As far as the reduction of the computational cost is concerned, it has to be stressed that the speed-up of the eventual morphodynamic simulations increases, i.e. the computational cost decreases, as the block duration increases, by exceeding a value of 20. These large speed-up values are achieved by implementing the proposed procedure aimed to reduce the original wave time series. It must be underlined that the proposed method is very simple to implement and is characterized by a very low computational cost.

## CRediT authorship contribution statement

**Francesca Scipione:** Conceptualization, Methodology, Software, Validation, Formal analysis, Investigation, Data Curation, Writing - Original Draft, Writing - Review & Editing, Visualization. **Paolo De Girolamo:** Conceptualization, Methodology, Writing - Review & Editing, Project administration, Funding acquisition. **Myrta Castellino:** Conceptualization, Methodology, Writing - Review & Editing. **Davide Pasquali:** Conceptualization, Methodology, Writing - Review & Editing. **Daniele Celli:** Conceptualization, Methodology, Writing - Review & Editing. **Marcello Di Risio:** Conceptualization, Methodology, Supervision, Software, Investigation, Writing - Review & Editing, Project administration.

## Acknowledgments

This research was partially funded by the "Ministero della Transizione Ecologica" (Italian Ministry for the Ecological Transition) within the frame of the "morfRESTORE" research project (Development of a novel one-line model for the analysis of the long-term evolution of sandy beaches and its application for the optimization of the management of the coastal stretch between Capo d'Anzio and Circeo aimed to the conservation of the beach and of the coastal dune of the National Park of Circeo - Director Decree 526-29/11/2017).

## References

Antolínez, J.A.A., Méndez, F.J., Camus, P., Vitousek, S., González, E.M., Ruggiero, P., Barnard, P., 2016. A multiscale climate emulator for long-term morphodynamics (muscle-morpho). Journal of Geophysical Research: Oceans 121, 775–791.

Bagnold, R., 1963. Mechanics of marine sedimentation. The sea 3, 507–528.

Bailard, J.A., Inman, D.L., 1981. An energetics bedload model for a plane sloping beach: local transport. Journal of Geophysical Research: Oceans 86, 2035–2043.

Battjes, J.A., Groenendijk, H.W., 2000. Wave height distributions on shallow foreshores. Coastal engineering 40, 161–182.

Battjes, J.A., Janssen, J., 1978. Energy loss and set-up due to breaking of random waves, in: Coastal engineering 1978. ASCE Library, pp. 569–587.

Baykal, C., Ergin, A., Güler, I., 2012. An energetic type model for the cross-shore distribution of total longshore sediment transport. Coastal Engineering , 2.

Beltrami, G.M., Bellotti, G., Girolamo, P.D., Sammarco, P., 2001. Treatment of wave breaking and total absorption in a mild-slope equation fem model. Journal of waterway, port, coastal, and ocean engineering 127, 263–271.

Benedet, L., Dobrochinski, J., Walstra, D., Klein, A., Ranasinghe, R., 2016. A morphological modeling study to compare different methods of wave climate schematization and evaluate strategies to reduce erosion losses from a beach nourishment project. Coastal engineering 112, 69–86.

Besio, G., Briganti, R., Romano, A., Mentaschi, L., De Girolamo, P., 2017. Time clustering of wave storms in the mediterranean sea. Natural Hazards and Earth System Sciences 17, 505–514.

Bodge, K.R., 1989. A literature review of the distribution of longshore sediment transport across the surf zone. Journal of Coastal Research , 307–328.

Bruun, P., 1983. Beach scraping—is it damaging to beach stability? Coastal Engineering 7, 167–173.

Camus, P., Mendez, F.J., Medina, R., 2011a. A hybrid efficient method to downscale wave climate to coastal areas. Coastal Engineering 58, 851–862.

Camus, P., Mendez, F.J., Medina, R., Cofiño, A.S., 2011b. Analysis of clustering and selection algorithms for the study of multivariate wave climate. Coastal Engineering 58, 453–462.

Capobianco, M., Hanson, H., Larson, M., Steetzel, H., Stive, M., Chatelus, Y., Aarninkhof, S., Karambas, T., 2002. Nourishment design and evaluation: applicability of model concepts. Coastal Engineering 47, 113–135.

Celli, D., Li, Y., Ong, M.C., Di Risio, M., 2019. The role of submerged berms on the momentary liquefaction around conventional rubble mound breakwaters. Applied Ocean Research 85, 1–11.

Celli, D., Pasquali, D., De Girolamo, P., Di Risio, M., 2018. Effects of submerged berms on the stability of conventional rubble mound breakwaters. Coastal Engineering 136, 16–25.

Celli, D., Pasquali, D., Fischione, P., Di Nucci, C., Di Risio, M., 2021. Wave-induced dynamic pressure under rubble mound breakwaters with submerged berm: An experimental and numerical study. Coastal Engineering 170, 104014.

Chesher, T., Miles, G., 1992. The concept of a single representative wave for sediment transport predictions. 1992) Hydraulic and Environmental Modelling: Coastal Waters. Proceedings on Hydraulic and Environmental Modelling of Coastal, Estuarine and River Waters. Ashgate Publishing Limited .

Chonwattana, S., Weesakul, S., Vongvisessomjai, S., 2005. 3d modeling of morphological changes using representative waves. Coastal Engineering Journal 47. doi:10.1142/S0578563405001240.

Ciccaglione, M.C., Buccino, M., Di Paola, G., Tuozzo, S., Calabrese, M., 2021. Trigno river mouth evolution via littoral drift rose. Water 13, 2995.

Cooper, J.A.G., Pilkey, O.H., 2004. Sea-level rise and shoreline retreat: time to abandon the bruun rule. Global and planetary change 43, 157–171.

Creter, R., Garaffa, T., Schmidt, C., 1994. Enhancement of beach fill performance by combination with an artificial submerged reef system, in: Proc. 7th National Conference on Beach Preservation Technology. Florida Shore and Beach Preservation Association, Tallahassee, FL, pp. 69–89.

CUR, 1987. Manual on artificial beach nourishment. Centre for Civil Eng Research, Codes and Specifications, Gouda, Rep 130.

Dally, W.R., Dean, R.G., Dalrymple, R.A., 1985. Wave height variation across beaches of arbitrary profile. Journal of Geophysical Research: Oceans 90, 11917–11927.

Daly, C.J., Bryan, K.R., Gonzalez, M.R., Klein, A.H., Winter, C., 2014. Effect of selection and sequencing of representative wave conditions on process-based predictions of equilibrium embayed beach morphology. Ocean Dynamics 64, 863–877.

Damiani, L., Aristodemo, F., Saponieri, A., Verbeni, B., Veltri, P., Vicinanza, D., 2011. Full-scale experiments on a beach drainage system: hydrodynamic effects inside beach. Journal of Hydraulic Research 49, 44–54.

Dean, R.G., 1977. Equilibrium beach profiles: US Atlantic and Gulf coasts. Department of Civil Engineering and College of Marine Studies, University of Newark, Delaware.

Deltares, 2011. Unibest-cl+ manual: Manual for version 7.1 of the shoreline model unibest-cl.

Di Risio, M., Lisi, I., Beltrami, G., De Girolamo, P., 2010. Physical modeling of the cross-shore short-term evolution of protected and unprotected beach nourishments. Ocean Engineering 37, 777–789.

U.S. Army Corps of Engineers, I., 1984. Shore Protection Manual. Government Printing Office,Washington,DC.

Fischione, P., Pasquali, D., Celli, D., Di Nucci, C., Di Risio, M., 2022. Beach drainage system: A comprehensive review of a controversial soft-engineering method. Journal of Marine Science and Engineering 10, 145.

Goda, Y., 2013. Empirical formulation of sediment pickup rate in terms of wave energy flux dissipation rate. Coastal Engineering Journal 55, 1350012.

Hallermeier, R.J., 1978. Uses for a calculated limit depth to beach erosion, in: Coastal Engineering 1978. Elsevier, pp. 1493–1512.

Hallermeier, R.J., 1980. A profile zonation for seasonal sand beaches from wave climate. Coastal engineering 4, 253–277.

Hanson, H., 1989. Genesis: a generalized shoreline change numerical model. Journal of Coastal research , 1–27.

Hersbach, H., Bell, B., Berrisford, P., Hirahara, S., Horányi, A., Muñoz-Sabater, J., Nicolas, J., Peubey, C., Radu, R., Schepers, D., et al., 2020. The era5 global reanalysis. Quarterly Journal of the Royal Meteorological Society 146, 1999–2049.

Holthuijsen, L., Booij, N., Ris, R., 1993. A spectral wave model for the coastal zone, in: Ocean wave measurement and analysis, ASCE. pp. 630–641.

Hurst, M.D., Barkwith, A., Ellis, M.A., Thomas, C.W., Murray, A.B., 2015. Exploring the sensitivities of crenulate bay shorelines to wave climates using a new vector-based one-line model. Journal of Geophysical Research F: Earth Surface 120. doi:10.1002/2015JF003704.

Kamphuis, J.W., 1991. Alongshore sediment transport rate. Journal of Waterway, Port, Coastal, and Ocean Engineering 117. doi:10.1061/(asce)0733-950x(1991)117:6(624).

Larson, M., Hanson, H., Kraus, N.C., 1987. Analytical Solutions of the One-Line Model of Shoreline Change. Technical Report. COASTAL ENGINEERING RESEARCH CENTER VICKSBURG MS.

Lee, K.H., Cho, Y.H., 2021. Simple breaker index formula using linear model. Journal of Marine Science and Engineering 9, 731.

Liu, Y., Niu, X., Yu, X., 2011. A new predictive formula for inception of regular wave breaking. Coastal Engineering 58, 877–889.

Long, J.W., Plant, N.G., 2012. Extended kalman filter framework for forecasting shoreline evolution. Geophysical Research Letters 39.

Malliouri, D.I., Petrakis, S., Vandarakis, D., Moraitis, V., Goulas, T., Hatiris, G.A., Drakopoulou, P., Kapsimalis, V., 2023. A chronology-based wave input reduction technique for simulations of long-term coastal morphological changes: An application to the beach of mastichari, kos island, greece. Water 15, 389.

Pasquali, D., Marucci, A., 2021. The effects of urban and economic development on coastal zone management. Sustainability 13, 6071.

Pelnard-Considére, R., 1956. Essai de theorie de lá evolution des formes de rivage en plages de sable et de galets. Journées de l'hydraulique 4, 289–298.

Plecha, S., Sancho, F., Silva, P., Dias, J.M., 2007. Representative waves for morphological simulations. Journal of Coastal Research .

Saponieri, A., Valentini, N., Di Risio, M., Pasquali, D., Damiani, L., 2018. Laboratory investigation on the evolution of a sandy beach nourishment protected by a mixed soft–hard system. Water 10, 1171.

Scipione, F., 2022. A novel one-line model for long-term evolution of sandy beaches in presence of coastal defence measures. Ph.D. thesis. "Sapienza" University of Rome.

Smith, E.R., Wang, P., 2002. Longshore sediment transport as a function of energy dissipation, in: Ocean Wave Measurement and Analysis (2001). ASCE Library, pp. 1218–1227.

Southgate, H.N., 1995. The effects of wave chronology on medium and long term coastal morphology. Coastal Engineering 26, 251–270.

Stauble, D.K., Tabar, J.R., 2003. The use of submerged narrow-crested breakwaters for shoreline erosion control. Journal of Coastal Research , 684–722.

Steijn, R., 1989. Schematization of the natural conditions in multi-dimensional numerical models of coastal morphology. Delft Hydraulics, Rept. H526-1 .

Steijn, R., 1992. Input filtering techniques for complex morphological models. Delft Hydraulics Laboratory.

Vitousek, S., Barnard, P.L., Limber, P., Erikson, L., Cole, B., 2017. A model integrating longshore and cross-shore processes for predicting long-term shoreline response to climate change. Journal of Geophysical Research: Earth Surface 122. doi:10.1002/2016JF004065.

de Vriend, H.J., Capobianco, M., Chesher, T., De Swart, H.d., Latteux, B., Stive, M., 1993. Approaches to long-term modelling of coastal morphology: a review. Coastal engineering 21, 225–269.

Walstra, D., Hoekstra, R., Tonnon, P., Ruessink, B., 2013. Input reduction for long-term morphodynamic simulations in wave-dominated coastal settings. Coastal Engineering 77, 57–70.

Walton, T.L., Dean, R.G., 1973. Application of littoral drift roses to coastal engineering problems, in: Proceedings of the Conference on Engineering Dynamics in the Surf Zone, Sydney, Australia.

Walton, T.L., Dean, R.G., 2010. Longshore sediment transport via littoral drift rose. Ocean Engineering 37, 228–235.

Yates, M., Guza, R., O'reilly, W., 2009. Equilibrium shoreline response: Observations and modeling. Journal of Geophysical Research: Oceans 114.

Highlights

**Reduced wave time series for long-term morphodynamic applications**

Francesca Scipione, Paolo De Girolamo, Myrta Castellino, Davide Pasquali, Daniele Celli, Marcello Di Risio

- Representative wave time series are crucial for long-term morphodynamic simulations
- Reduced time series allow saving computational time
- An effective method to reduce offshore wave series is proposed
- Reduced series can be effectively used for long-term morphodynamic simulations

# Reduced wave time series for long-term morphodynamic applications

*by Scipione, F., De Girolamo, P., Castellino, M., Pasquali, D., Celli, D., Di Risio, M.*

## CRediT authorship contribution statement

**Francesca Scipione:** Conceptualization, Methodology, Software, Validation, Formal analysis, Investigation, Data Curation, Writing - Original Draft, Writing - Review & Editing, Visualization. **Paolo De Girolamo:** Conceptualization, Methodology, Writing - Review & Editing, Project administration, Funding acquisition. **Myrta Castellino:** Conceptualization, Methodology, Writing - Review & Editing. **Davide Pasquali:** Conceptualization, Methodology, Writing - Review & Editing. **Daniele Celli:** Conceptualization, Methodology, Writing - Review & Editing. **Marcello Di Risio:** Conceptualization, Methodology, Supervision, Software, Investigation, Writing - Review & Editing, Project administration.

**Declaration of interests**

☒ The authors declare that they have no known competing financial interests or personal relationships that could have appeared to influence the work reported in this paper.

☐The authors declare the following financial interests/personal relationships which may be considered as potential competing interests: